Accepted Manuscript

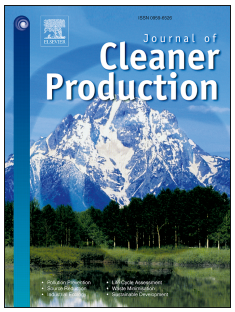

Extremely fast and efficient methylene blue adsorption using eco-friendly cork and paper waste-based activated carbon adsorbents

Rui M. Novais, Ana P.F. Caetano, Maria P. Seabra, João A. Labrincha, Robert C. Pullar

PII: S0959-6526(18)31937-1

DOI: 10.1016/j.jclepro.2018.06.278

Reference: JCLP 13424

To appear in: *Journal of Cleaner Production*

Received Date: 2 May 2018

Revised Date: 25 June 2018

Accepted Date: 27 June 2018

Please cite this article as: Novais RM, Caetano APF, Seabra MP, Labrincha JoãA, Pullar RC, Extremely fast and efficient methylene blue adsorption using eco-friendly cork and paper waste-based activated carbon adsorbents, *Journal of Cleaner Production* (2018), doi: 10.1016/j.jclepro.2018.06.278.

Extremely fast and efficient methylene blue adsorption using eco-friendly cork and paper waste-based activated carbon adsorbents

Rui M. Novais [a,*], Ana P.F. Caetano [a], Maria P. Seabra [a], João A. Labrincha [a], Robert C. Pullar [a]

[a] Department of Materials and Ceramic Engineering / CICECO- Aveiro Institute of Materials, University of Aveiro, Campus Universitário de Santiago, 3810-193 Aveiro, Portugal

*Corresponding author: Tel.: +351234370262; fax: +351234370204

E-mail address: ruimnovais@ua.pt (Rui M. Novais)

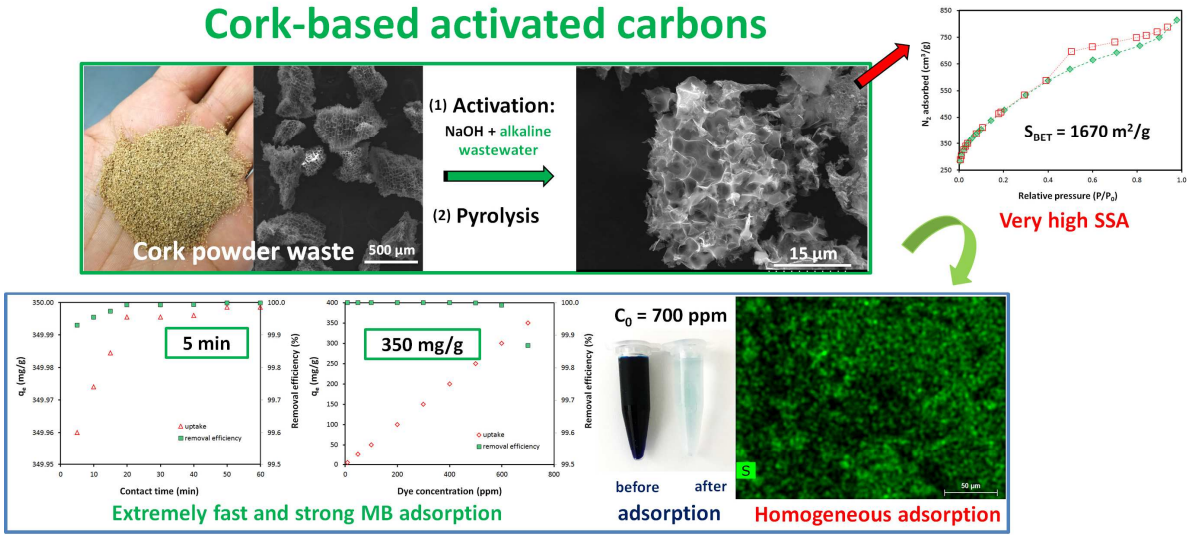

Abstract

For the first time the feasibility of using an alkaline wastewater coming from the pulp and paper industry as an activator, partially (50 vol.%) replacing commercial sodium hydroxide, in the production of cork-based activated carbons was evaluated. The activated carbons showed the highest value of specific surface area ever reported for cork-based activated carbons (1670 m^2/g), surpassing several other commercial and waste-based ones. These eco-friendly cork and paper waste-based activated carbons were then evaluated as methylene blue adsorbent materials. The influence of contact time, methylene blue initial concentration and adsorbent amount on the methylene blue removal efficiency by the activated carbons was studied. Extremely fast (>99.9 % removal in 5 min) and efficient methylene blue adsorption (uptake of 350 mg/g) by the cork and paper waste-based adsorbents was achieved, which demonstrates the huge potential of these innovative adsorbents. These activated carbons were produced using two unexplored industrial by-products (alkaline wastewater and cork) and, therefore, may be an inexpensive source of activated carbons, which can be used for the effective removal of dyes from wastewaters. Furthermore, despite the very large surface area and high removal efficiency this is ***not*** a nano material (being around 30-50 μm in size), its capabilities being due to its unique cork-derived microstructure, and hence it can be handled and removed/filtered much more easily than nanocarbons, and without any associated health or environmental risks.

Keywords: cork-based activated carbon; industrial wastewater; dye adsorption; equilibrium isotherm; biochar.

1. Introduction

Annually industrial dyeing processes release between 30,000 and 150,000 t of dyes into wastewaters (Anjaneya *et al.*, 2013), raising serious environmental concerns due to the toxicity and carcinogenic properties of most of these dyes. This further intensifies clean water scarcity, which is already seen as one of the most pressing concerns of our society (World Economic Forum, 2016). Wastewater treatment is, therefore, of the utmost importance, and may provide a very important source of clean drinking water. Various methods have been used to remove dyes from wastewaters. Nevertheless, adsorption is considered the most effective and simple method for water decontamination (Rafatullah *et al.*, 2010).

This technique does not generate harmful intermediate products, this being a major advantage over other techniques such as photodegradation/photocatalysis. These features explain the great number of investigations addressing adsorption (Arabi *et al.*, 2017) in comparison with other techniques. Activated carbons present singular properties, such as their high specific surface area (SSA) and adsorption capacity, and as such are one of the most commonly used adsorbents. Nevertheless, their high production cost hinders their widespread use (Rafatullah *et al.*, 2010). Waste materials may be an inexpensive source of activated carbons which could allow the spread of this technology. Activated carbons have been prepared using a wide variety of waste, such as spent coffee grounds (Ma and Ouyang, 2013), waste carbon (Cheng *et al.*, 2017), *ficus carica* bast (Pathania *et al.*, 2017), palm shell (Wong *et al.*, 2016), among others.

Cork is a renewable and sustainable material extracted from the outer bark of the cork oak tree (*Quercus Suber L.*), and Portugal is the world's largest cork producer (~ 50 %) (APCOR, 2016). Cork is fully sustainable, as the tree is not harmed during harvesting every 10 years, living on as a carbon sink for 200-300 years, and the equivalent of any

CO_2 realised from the cork during processing will be absorbed by the tree to produce the next growth of bark. This is a very relevant advantage over other carbonaceous materials contributing towards cleaner production. Cork has singular properties such as exceptional thermal, acoustic and vibrational insulation, which allows its use in applications ranging from construction and transports to sports. Nevertheless, the main application for cork is as wine stoppers. Cork powder is the main waste of the cork industry, being generated throughout the fabrication stages of various cork products (Atanes *et al.*, 2012). In the granulation process, for manufacturing black and white agglomerated cork construction products and granules, around 35 % of cork powder is produced (Demertzi *et al.*, 2016), with an annual production estimated to reach around 50,000 t (Cardoso *et al.*, 2008). This residue has low economic value, and for that reason it has been mainly used for energy generation through its combustion (Demertzi *et al.*, 2016). However, recent studies have demonstrated the possibility of using cork waste as a precursor in the preparation of activated carbons. Cabrita *et al.* (2010) studied the removal of acetaminophen (an analgesic) from water, while Cardoso *et al.* (2008) evaluated the feasibility of using cork-based activated carbons to control atmospheric pollution. This exciting strategy may attribute value to this industrial waste. Cork's unique microstructure, consisting of hollow polyhedral cells (~20 μm diameter) and containing up to 200 million cells per cm^3 (Pereira, 2007), could lead to very high surface area materials and low water content (energy saving) (Aroso *et al.*, 2017), these being crucial advantages over other carbonaceous materials. Waste cork-based activated carbons may be a low-cost and sustainable alternative to the use of commercial activated carbons. This could be particularly relevant to the Portuguese context, since 34 % of worldwide cork oak forest is located in Portugal (Gil, 2014), responsible for 50 % of global cork production. Cork-based activated carbons have been used as

adsorbents to remove volatile organic compounds (Cardoso *et al.*, 2008) and emergent pollutants (Mestre *et al.*, 2014).

However, despite their promising results, commercial alkaline activators such as KOH or K_2CO_3 were used in these previous investigations to prepare the activated carbons. These additives are detrimental to the activated carbon production cost and carbon footprint. In the little literature which exists addressing the synthesis of cork-based activated carbons, only KOH (Atanes *et al.*, 2012), K_2CO_3 (Carvalho *et al.*, 2004) and phosphoric acid (Aroso *et al.*, 2017) have been used as activation agents. Here, an innovative and more eco-friendly strategy was implemented, in which a mixture of an alkaline industrial wastewater (coming from the local Portuguese pulp and paper industry) and sodium hydroxide was used to produce cork-based activated carbons. This is the first ever report of the production of cork-based activated carbons using an alkaline waste for the chemical activation of the cork. The use of this industrial wastewater instead of virgin raw materials (e.g. sodium hydroxide) may reduce the activated carbons production cost and carbon footprint in comparison with those produced solely using commercial activating agents, while simultaneously mitigating the amount of wastewater disposal from the paper industry.

The adsorbents prepared were then used to extract methylene blue (MB) from synthetic wastewaters, which to the best of our knowledge has never been reported for cork-based activated carbons. MB is a well-known monovalent cationic synthetic dye used in different fields (e.g. medicine, chemistry and industry), which is known to be toxic to humans (Novais *et al.*, 2018) as well as the environment, and, therefore, its presence in wastewaters is highly undesirable, and its removal mandatory (Rafatullah *et al.*, 2010).

In this investigation, cork-based activated carbons exhibiting very high surface area (~ 1670 m^2/g) were first produced using a waste-based activator, and then evaluated as MB

adsorbent material. The influence of MB initial concentration, contact time and adsorbent concentration on the MB removal efficiency and uptake by the cork-based activated carbon was studied. Results demonstrate the feasibility of using significant amounts of an unexplored industrial alkaline waste (50 vol.%) to replace commercial activators (e.g. sodium hydroxide) in the production of eco-friendly and sustainable cork-based activated carbons, showing very high and fast MB removal capacity. This innovative strategy reduces the activated carbon production cost in comparison with those produced using solely commercial chemicals (the alkaline wastewater has currently no commercial value, being considered a waste) while simultaneously attributing value to two distinct waste streams (wastewater effluent and cork residues), and mitigating the environmental impacts associated with the wastes disposal.

2. Materials and methods

2.1. Materials

The cork powder waste was supplied by a Portuguese cork industry (Amorim). This waste, produced during the cork granulation process, has a bulk density of 50-70 kg/m^3, and the particles are in the range of ~0.5-1 mm in dimension.

The cork activation was performed using a mixture of 10 M sodium hydroxide (ACS reagent, 97 %; Sigma Aldrich) and alkaline wastewater (effluent; pH ~ 11.5) generated during the Kraft process in a Portuguese pulp and paper plant. The activators were used in a 50:50 vol.% proportion. This ratio between the activators was selected considering preliminary tests, which showed a significant drop in the SSA when using higher wastewater contents.

MB with the molecular formula: $C_{16}H_{18}ClN_3S$, supplied by Sigma Aldrich, was used as adsorbate. To prepare the various MB solutions distilled water was used as solvent. The stock solutions were sealed with an aluminium foil and kept in dark conditions until the adsorption tests, to prevent any possible photodegradation.

2.2. Activated cork synthesis

As-received cork powder was added to the alkaline solution (NaOH:alkaline wastewater) and then magnetically stirred at room temperature for 2 h, following a previous work (Mestre *et al.*, 2014). The solid-to-liquid ratio was kept constant (0.8 g cork / 50 mL solution). Future work will address the influence of the activating solution dosage on the textural properties of the activated carbons aiming to reduce the dosage, and, therefore, the carbon footprint of the activated carbons. After filtration (Nylon net; PA 15/11 L=1050) and drying (12 h at 80 ºC) the cork was placed in graphite crucibles, and then pyrolysed under nitrogen in a graphite furnace. The following cycle was used: i) 5 ºC/min heating rate up to 150 ºC; (ii) 10 ºC/min heating rate up to 900 ºC; iii) 30 min dwell time at this temperature; and (iv) cooling (at 10 ºC/min) to room temperature. The pyrolysis cycle was selected considering previous works by the authors (Pullar *et al.*, 2015; Pullar and Novais, 2017) in which cork wastes were used as a template in the production of ecoceramics. The pyrolysed activated cork (AC) was washed with distilled water until neutral pH and dried in the oven at 80 °C. Prior to their use as adsorbents, the AC samples were sieved, and then only particles below 75 μm were used.

2.3. Methylene blue adsorption tests

Adsorption experiments were carried out at room temperature (20 ºC) to decrease the process energy costs, and to be closest to the industrial context. The influence of contact time, MB initial concentration and AC concentration on the MB uptake by the AC adsorbent were evaluated. Various AC amounts (2.0-3.5 g/L) were added to 5 mL of a solution containing a specific MB concentration (10-700 ppm) and magnetically stirred during a pre-determined period (5-60 min). At least two replicates of each condition were tested and the average values presented. After adsorption tests the samples were filtered and the MB concentration in the liquid was evaluated by UV spectroscopy (Shimadzu UV-3100, JP) by measuring the absorbance at a λ = 664 nm. Prior to these measurements, a calibration curve for MB was performed. The following regression equation was obtained: Y = 6.29 X (r^2 = 0.996), where Y corresponds to the MB concentration and X to the absorbance.

Two parameters were calculated to evaluate the MB removal by the AC, the uptake (q_e) in mg/g, and the removal efficiency percentage (E), using equation 1 and 2:

$$q_e = \frac{(C_0 - C_e)}{m} \times V \quad (1)$$

$$\mathrm{E}\ (\%) = \frac{\mathrm{C_0} - \mathrm{C_e}}{\mathrm{C_0}} \times 100 \quad (2)$$

where the initial MB concentration (mg/L) is given by C_0, the MB remaining equilibrium concentration (mg/L) by C_e, the solution volume by V (L) and the adsorbent mass (g) by m.

Two adsorption isotherm models were used to fit the experimental results, namely Langmuir and Freundlich. The Lagmuir model is described by the equation:

$$\frac{1}{\mathrm{q_e}} = \frac{1}{\mathrm{K_L q_{max} C_e}} + \frac{1}{\mathrm{K_L}} \quad (3)$$

where K_L is the affinity of the sorbate for the binding sites (L/mg) and q_{max} the maximum adsorption capacity (mg/g).

The Freundlich model is described by equation (4):

$$logq_e = logK_F + \frac{1}{n} logC_e \quad (4)$$

2.4. Materials characterisation and analysis

AC zeta-potential was assessed with a Zetasizer Nano ZS (Malvern) using a deionised water suspension at room temperature.

The specific surface area of the AC adsorbent was determined using the Brunauer-Emmett-Teller (BET) method by N_2 adsorption using a 5-point BET method on a Micromeritics Gemini 2380 surface area analyser. The sample was outgassed at 150 ºC. The microporous properties (volume and surface area) were estimated using the t-plot method (Galarneau *et al.*, 2014).

Scanning electron microscopy (SEM) coupled with energy dispersive spectroscopy (EDS - Rontec) analysis, performed using a Hitachi S4100 system with electron beam energy of 25 KeV, was used to study the AC adsorbent microstructure. EDS maps of the AC before and after MB adsorption were carried out using a Hitachi SU-70 SEM.

Thermogravimetic–differential scanning calorimetry (TG-DSC) analyses were used to survey the thermal behaviour of the samples before and after MB adsorption, which were carried out with a Setaram Setsys Evolution 1750 in TG-DSC mode (Type S sensor) equipped with an alumina plate under air flow at 200 mL/min, and samples were heated at 10 °C/min up to 900 °C.

The adsorbent particle size distribution was evaluated by laser diffraction (Coulter LS230 analyser).

Contact angle measurements were carried out in a Contact Angle System OCA 15, at room temperature, using 1 droplet of water in each sample. The measurements were performed after 3 s of contact between the droplet and the cork surface, and repeated three times. For this test, AC powder was dry-pressed into discs using a stainless steel die (10 mm diameter).

Inductively coupled plasma (ICP) measurements were performed to evaluate the wastewater composition (Thermo Scientific iCAP 7000 Series).

Fourier-transform infrared spectroscopy (FT-IR) measurements, in attenuated total reflectance (ATR) mode, of the *as-received* cork and the cork-based activated carbon (prepared with 50 vol.% wastewater) were carried out in a Perkin Elmer FT-IR System Spectrum BX spectrophotometer equipped with a single horizontal Golden Gate ATR cell. The measurements were performed at room temperature using 4 cm^{-1} in resolution, 264 scans in a range between 4000 and 500 cm^{-1}.

3. Results and discussion

3.1. Precursors characterisation

A photograph and SEM micrographs of the cork powder waste are presented in Fig. 1. The cork powder is composed of irregular particles, sized between 400 µm and 1 mm, showing low specific surface area (8.2 m^2/g) (N_2 adsorption-desorption isotherms at 77 K presented in Fig. 2a) which is attributed to their closed cells. Untreated cork has very low open porosity, this being one of the reasons why this unique material floats in water and has low permeability. In line with this remark, the micropore surface area of the cork, estimated using the t-plot method, is 6.3 m^2/g.

The chemical composition of the alkaline wastewater, presented in Table S1 (Supplementary Material), reveals sodium as the major element, while minor amounts of silicon, aluminium and iron were also detected. Its chemical composition, associated with its high alkalinity (pH ~ 11.5), suggest the possibility of its use to partially replace commercial activators, such as potassium or sodium hydroxides, in the production of activated carbons. The feasibility of reusing the wastewater in multiple activation cycles will be evaluated in future work.

3.2. Activated cork characterisation

Fig. 3 shows typical SEM micrographs and EDS map of the produced AC, while some physical properties are presented in Table 1. The activation process induces severe changes in the AC microstructure in comparison with that of the *as-received* cork (see Fig. 1). The AC shows much higher porosity than the original precursor, with several holes being visible in the SEM micrographs. Fig. 3b and 3c clearly show the presence of a high number of open pores, absent in the non-activated cork. This is mainly attributed to the chemical activation process, while pyrolysis induces considerable weight reduction but does not significantly affect the cork's microstructure (Pullar *et al.*, 2015; Pullar and Novais, 2017). The resulting particles are between 30-50 μm in diameter.

The N_2 adsorption-desorption isotherms at 77 K, and the cumulative pore volume of the AC, are presented in Fig. 2c and 2d. Results show that the AC exhibit typical type IV isotherms (Sing *et al.*, 1985), which are characteristic of mesoporous materials. For these materials, an increase in the relative pressure induces a significant uptake on the adsorbed N_2. At low relative pressure monolayer adsorption occurs in the micropores, and then when the monolayer adsorption is complete, multilayer adsorption begins filling the mesopores (Beltrame *et al.*, 2018), with capillary condensation resulting in

the hysteresis loop observed. The cumulative pore volume (Fig. 2d) shows the presence of micropores and mesopores in the AC. Nevertheless, around 79 % of the pores in the AC are between 2 and 50 nm, which confirms the mesoporous nature of this material. Other relevant parameters such as the micropore surface area and micropore volume are presented in Table 1.

The chemical activation of cork, and subsequent pyrolysis, leads to the production of an AC with very high specific surface area (1670 m^2/g), which is highly advantageous for adsorption applications. As mentioned in section 2.1, higher wastewater to NaOH ratios were investigated for the chemical activation of cork. However, an increase on the wastewater content above 50 vol.% lead to a significant decrease in the SSA. For example, when using 75: 25 vol.% (wastewater:NaOH), the SSA dropped to around 888 m^2/g (see Fig. 2c), while the sole use of the effluent (100 vol.%) lead to very poorly activated carbons (SSA ~ 6 m^2/g). Future work will consider the optimisation of activation parameters (e.g. time and temperature) to allow the use of higher wastewater contents. In any case, results suggest that the nature of the produced pores (micro or mesopores) changes when the wastewater to NaOH ratio rises: the micropore volume rises from 0.06 to 0.27 cm^3/g when the wastewater volume increases from 50 to 75 vol.%. As a consequence, the percentage of mesopores drops from 79 % (in the composition prepared using 50:50 vol.%) to 59 % (75:25 vol.%).

Table 2 compares the SSA of the cork-based activated carbon produced here with values reported in previous studies. As can be seen, the value obtained here surpasses that of several other adsorbents, and is the highest ever reported for cork-derived activated carbon. This promising result is expected to assure high adsorption performance. Furthermore, the feasibility of using high amounts of an industrial alkaline

wastewater (50 vol.%) to partially replace benchmark activators (e.g. sodium hydroxide) in the production of AC with very high SSA is also demonstrated.

Fig. 4 presents the zeta potential evolution with pH variation for the synthesised AC. The adsorbent's zeta potential is positive when pH is below 3.6, sharply decreasing to negative values above the pH_{PZC}. This result shows that the surface of the adsorbent is negatively charged when the pH is above 3.6, reaching the highest charge density at pH around 12. At this pH, the maximum attraction between the adsorbent and the cationic MB dye will occur, favouring MB adsorption. The influence of the solution pH on MB removal efficiency has been previously investigated, with higher pH values favouring adsorption (Khan *et al.*, 2015; Qada *et al.*, 2006). In this study, the solution pH varies with the MB initial concentration, dropping from ~ 7 (distilled water) to 4.9 when the MB concentration reaches 700 ppm. pH values were always significantly lower than 12, while this value assures the greatest charge density on the adsorbent's surface (according to its zeta potential variation). This means it's already impressive removal capacity (described in section 3.3) could be further optimised by increasing the solution pH. This will be addressed in future work.

The AC adsorbent mean particle size (see Table 1) was found to be ~ 30 µm, with 90 % of its particles having sizes below 56 µm.

To further characterise the adsorbent properties, its contact angle was measured and the result included in Table 1. The AC has a contact angle of 34.9 º, which demonstrates that the chemical activation of cork and subsequent pyrolysis modifies the surface hydrophilicity, from highly hydrophobic (*as-received* cork waste) to highly hydrophilic/hydroxylic (AC). This feature will be highly advantageous for the application here envisioned (MB adsorption).

The FTIR spectra of the *as-received* cork and the activated carbon are shown in Fig. S1. Significant differences between tTGhe spectra are depicted, suggesting that chemical activation changes the materials' surface chemistry. After chemical activation, the suberin aliphatic bands (-CH_3 aliphatic stretching) detected in the *as-received* cork (~ 2925 and 2854 cm^{-1}) (Pintor *et al.*, 2012) are absent. Likewise, the features at around 1735 and 3394 cm^{-1}, assigned to C=O stretching in suberin, cellulose and hemicellulose (Pintor *et al.*, 2012) and to O–H stretching (mainly from water) (Pintor *et al.*, 2012), are not observed in the activated cork. These results confirm the modification of the cork's surface chemistry. The FTIR spectrum of the activated carbon shows an overlapping band at ~ 1637 cm^{-1}, belonging to the C=C stretching (Pintor *et al.*, 2013), and a broad band between 1508 and 1260 cm^{-1} typically associated with C-O vibrations from groups such as esters, carboxylic acids, carboxylic anhydrides, lactones, alcohols, ethers, phenols and carboxyl-carbonates (Pintor *et al.*, 2013).

3.3. Methylene blue adsorption tests

3.3.1. Influence of contact time

The high SSA of the synthesised AC adsorbent is expected to promote fast sorption of the MB molecules. Accordingly, the adsorption rate in the first 60 min was evaluated using constant AC amount (2 g/L) and MB initial concentration (700 ppm). This very high concentration was selected considering preliminary tests that showed outstanding performance of the adsorbent for lower MB concentrations. The AC amount (2 g/L) selected for this study is equivalent to that used in other studies (Naeem *et al.*, 2017; Raposo *et al.*, 2009), and is inferior to that used by Bestani *et al.* (2008) and Stavropoulos and Zabaniotou (2005), at 4 and 6 g/L. The influence of the adsorbent concentration will be discussed in section 3.3.3.

Fig. 5 shows the uptake and the adsorbent removal efficiency versus contact time for sorption time up to 60 min. Results denote strong and extremely fast adsorption of the dye by the AC: after 5 min the removal efficiency was 99.929 %, further increasing to 99.997 % after 60 min. The uptake showed similar trend, a threshold being reached after 20 min. The minor increase with time observed for the removal efficiency (0.068 %) and the uptake (0.004 mg/g) confirms the high speed of the process, and for that reason a contact time of 5 min can be considered as the equilibrium time. The possibility of using smaller contact times was not evaluated here, but will be considered in future work. The influence of contact time on the MB adsorption by geopolymer monoliths (Novais *et al.*, 2018) and activated carbons (Pathania *et al.*, 2017) has been previously investigated. The equilibrium time here reported (5 min) was compared with other literature studies and results are shown in Fig. 6. The equilibrium time achieved with the cork-based activated carbon is substantially quicker than those reported for mangosteen peels (300 min) (Nasrullah *et al.*, 2018), palm shell (200 min) (Wong *et al.*, 2016), loofah sponge (120 min) (Li *et al.*, 2018), ficus carica bast (60 min) (Pathania *et al.*, 2017), among others (Naeem *et al.*, 2017; Tran *et al.*, 2017); it is similar to that of nanoporous carbon produced from wheat straw (Han *et al.*, 2018). Nevertheless, those authors used $ZnCl_2$ in the activation step (Han *et al.*, 2018), whereas here a more sustainable approach was employed, involving the use of 50 vol.% of an industrial wastewater as activator. In any case, this remarkable result demonstrates a high affinity of the produced AC for the MB molecules, hence suggesting its use for effective wastewaters decontamination.

3.3.2. Influence of MB initial concentration

Fig. 7 illustrates the influence of MB initial concentration (C_0) on the MB removal efficiency and uptake by the AC. Results show excellent removal efficiency for all MB concentrations studied (between 10 and 700 ppm). The removal efficiency was 100 % for C_0 below 500 ppm, and then only slightly decreased reaching 99.87 % at $C_0 = 700$ ppm. The MB uptake by the AC substantially increases with the rise of C_0, reaching an impressive 350 mg/g when using $C_0 = 700$ ppm. This behaviour can be explained considered the mass transfer resistance between the liquid and the solid phase during adsorption, which is affected by C_0 value. An increase in the MB initial concentration boost the interactions between the MB molecules and the AC surface, providing a significant driving force for mass transfer between the adsorbate and the adsorbent, favouring adsorption. This behaviour is in line with other investigations addressing the use of nanoporous carbon (Han *et al.*, 2018) and waste rice activated carbon (Sangon *et al.*, 2018) adsorbents.

The maximum adsorption capacity here reported (350 mg/g) was compared with that reported for other MB adsorbents, and results are presented in Table 3. The cork-based activated carbon shows an outstandingly high adsorption capacity, surpassing several other commercial (Bestani *et al.*, 2008; Stavropoulos and Zabaniotou, 2005) and waste-based activated carbons, such as those prepared from waste carbon (Cheng *et al.*, 2017), mangosteen peels (Nasrullah *et al.*, 2018), loofah sponge (Li *et al.*, 2018), palm shell (Wong *et al.*, 2016), rice straw (Gao *et al.*, 2011), among others (Naeem *et al.*, 2017; Pathania *et al.*, 2017). The adsorption capacity of the AC produced here is only surpassed by those reported by Sangon *et al.* (2018), Han *et al.* (2018) and Qada *et al.* (2006). However, in these investigations more complex processes were employed: in Sangon *et al.* (2018) the activated carbon synthesis required two-step pyrolysis, while in

Han *et al.* (2018) $ZnCl_2$ (activator) and a HF solution (to remove metallic species and silica) were used, and in Qada *et al.* (2006) a very high equilibrium time (3 weeks) and pH control (pH = 11) were adopted.

On the contrary, here a one-step pyrolysis, an activator consisting of 50 vol.% wastewater, and a much shorter contact time (10 min) were employed. Moreover, adsorption tests were performed at pH below 7, which suggests that further enhancement is feasible simply modifying the solution pH. In other words, our approach seems to be more cost-effective (does not require two heat treatments, or the sole use of commercial activators) and environmentally friendly (uses an industrial wastewater as activator and cork waste for carbon). Nevertheless, the economic advantage of the proposed strategy must be supported by a full cost-benefit analysis. This topic will be addressed in future work, but is beyond the scope of this article.

Additionally, MB adsorption tests were performed at room temperature (20 ºC), while the values (included in Table 3) reported by Cheng *et al.* (2017), Li *et al.* (2018) and Pathania *et al.* (2017) were measured at 50 ºC, 30 ºC and 30 ºC. Adsorption of MB onto activated carbons is known to be favoured by the increase in temperature (Li *et al.*, 2018; Pathania *et al.*, 2017). Therefore, an increase of the cork-based adsorbents' removal capacity is to be expected with increasing temperature, which further validates the potential of the cork-based activated carbons synthesised in this work.

3.3.3. Influence of the AC concentration

The influence of the adsorbent amount on the MB removal efficiency and uptake is illustrated in Fig. 8. The use of 2 g/L induces very high removal efficiency (99.954 %). Increasing the AC concentration further improves the MB removal up to 99.999 % when using 3.5 g/L. Obviously, the MB uptake by the AC drops when AC content

increases, which was expected from the analysis of equation (1). Despite the slight increase in the removal efficiency, observed when increasing the AC amount, the use of 2 g/L seems to be the most cost-effective solution with no significant drop in performance.

3.3.4. Characterisation of the AC after MB adsorption

To characterise the AC after MB adsorption tests, SEM analysis was carried out, and the corresponding EDS maps of the adsorbent is presented in Fig. 9. The presence of sulphur (identified in green in the EDS map), not present in the AC before adsorption, was considered as evidence of MB adsorption by the AC. The EDS maps show that sulphur, and therefore MB, is homogeneously distributed throughout the AC, which suggests homogeneous binding sites and equivalent sorption energy on the adsorbent surface. This will be further discussed in section 3.3.5 (adsorption isotherm studies).

Fig. 10 shows the TG-DSC curves of the AC before and after MB adsorption. The derivative of the TG curve for the AC shows two degradation steps at ~385 and 475 ºC, coinciding with the exothermic peaks shown in the DSC curve (Fig. 10b). The TG curve also shows that the thermal decomposition of the AC structure is almost completed at temperatures around 500 ºC. Interestingly, after MB adsorption the thermal stability of the AC increases, as demonstrated by the TG curve. A single peak is observed in the derivative of the TG curve at ~ 555 ºC, while the complete decomposition is delayed almost 100 ºC in comparison with the AC curve before MB adsorption. The increase in the thermal stability was associated with the presence of MB. The DTA curve of this dye (not shown here for the sake of brevity) shows several exothermic peaks/bands, at 180, 275, 390 and 520 ºC connected to the thermal decomposition of the dye, thus explaining the higher thermal stability of the AC after MB adsorption.

3.3.5. Adsorption isotherm studies

To understand the adsorption mechanism by the AC, the experimental results were fitted using Freundlich and Langmuir adsorption models. Figure 11 presents the AC uptake vs the MB equilibrium concentration, as well as the fitting using the Langmuir and the Freundlich models, while the adsorption parameters, calculated according to equations (3) and (4), are presented in Table 4. The uptake value increases in a non-linear fashion, reaching saturation conditions at higher equilibrium concentration (C_e).

The Freundlich model assumes that sorption occurs on a heterogeneous surface, where stronger binding sites are occupied first and the binding strength decreases with increasing degree of occupation (Kim, 2015). The *n* parameter, known as heterogeneity factor, indicates whether the adsorption is linear (n = 1), chemical (n < 1) or if a physical process is favourable (n > 1) (Vargas *et al.*, 2011). A high correlation coefficient (R^2) was obtained with the Freundlich isotherm (0.979), which indicates the applicability of the model. The slope of the curve log q_e versus log C_e given by the parameter 1/n is < 1 (1/n = 0.066), suggesting a strong interaction between the adsorbate and the adsorbent (Febrianto *et al.*, 2009). The value of n = 15.08 also indicates that the physical process is favourable.

The Langmuir model assumes homogeneous binding sites and equivalent sorption energy in the surface (Kim, 2015). The correlation coefficient obtained from this isotherm (R^2 = 0.902) is lower than that observed for the Langmuir model. Nevertheless, a very high affinity of the sorbate for the binding sites (K_L) was observed, while the separation factor (R_L) calculated from Langmuir isotherm (see details in (Novais *et al.*, 2018)) is between 0 and 1, suggesting that there is favourable adsorption. The decrease in R_L when rising the MB initial concentration indicates that adsorption is more favourable at higher concentrations (Vargas *et al.*, 2011). This model predicts a

homogeneous adsorption occurring between the adsorbent surface, which is in line with the EDS maps (see Fig. 9) performed after MB adsorption which showed a homogeneous distribution of sulphur, and therefore of MB, on the AC surface. According to the Langmuir isotherm, the adsorbents sorption capacity (q_m) is 333.33 mg/g, reasonably close to the maximum experimental uptake value achieved here (350 mg/g). For these reasons, the Langmuir model was considered the most suitable for describing the MB adsorption mechanism by the AC.

4. Conclusions

In this work, and for the first time, the feasibility of using an alkaline industrial wastewater (pH ~ 11.5) as a partial replacement for commercial activating solutions in the synthesis of cork-based activated carbons was investigated. Cork residues have been successfully activated by using a mixture of sodium hydroxide and alkaline wastewater (50 vol.%), leading to the production of mesoporous activated carbon with very high specific surface area (1670 m^2/g), surpassing all previous investigations regarding the production of cork-based activated carbons. Higher wastewater to NaOH ratios were investigated for the chemical activation of cork. However, an increase in the wastewater content above 50 vol.% lead to a significant decrease in the SSA. Future work will consider the optimisation of activation parameters to allow the use of higher wastewater contents. It should be pointed out that, despite the very large surface area and high removal efficiency of this material, it is ***not*** a nano material (being around 30-50 μm in size), its capabilities being due to its unique cork-derived microstructure. Therefore, it can be handled and removed/filtered much more easily than any nanocarbons, while also avoiding associated health or environmental risks.

The AC exhibiting the highest SSA was then evaluated as an adsorbent material for methylene blue. This is the first report considering the use of cork-based activated carbons for methylene blue extraction from wastewaters. Results showed rapid (removal of >99.9% in 5 min) and high (350 mg/g uptake) MB extraction by the AC. The remarkable MB adsorption capacity, in comparison with other literature results, demonstrates the interesting potential of this wastes-activated, cork-based AC for dyes removal from wastewaters.

In this investigation, cork, an exceptionally sustainable and renewable material, was used as precursor, and an alkaline wastewater was used as activator, which further decreases the activated carbon production cost and carbon footprint in comparison with those produced using solely commercial chemicals. Nevertheless, a full cost-benefit analysis must be performed in the future to demonstrate the absolute economic advantage of the proposed strategy. This will be considered in future work. Future work will also address the use of the cork-based activated carbon in the treatment of real wastewaters, instead of synthetic ones, where the influence of co-existing ions must be considered. Furthermore, the influence of the cork wastes variability on the activated carbon properties should also be investigated.

Acknowledgements: This work was developed within the scope of the project CICECO-Aveiro Institute of Materials, POCI-01-0145-FEDER-007679 (FCT Ref. UID /CTM /50011/2013), financed by national funds through the FCT/MEC and when appropriate co-financed by FEDER under the PT2020 Partnership Agreement. R.C. Pullar wishes to thank FCT grant IF/00681/2015 for supporting this work, and R.M. Novais wishes to thank FCT project H2CORK (PTDC/CTM-ENE/6762/2014).

References

O. Anjaneya, S.S. Shrishailnath, K. Guruprasad, A.S. Nayak, S.B. Mashetty, T.B. Karegoudar **Decolourization of Amaranth dye by bacterial biofilm in batch and continuous packed bed bioreactor** International Biodeterioration & Biodegradation, 79 (2013), pp. 64-72

APCOR **Cork Yearbook 2016. Cork statistic report from the Portuguese Cork Association** (Portugal), (2016). Available from: www.apcor.pt/wp-content/uploads/2016/09/Boletim-estatistico-2016.pdf (accessed on 01.06.18).

M. Arabi, M. Ghaedi, A. Ostovan **Development of a lower toxic approach based on green synthesis of water-compatible molecularly imprinted nanoparticles for the extraction of hydrochlorothiazide from human urine** ACS Sustainable Chemistry & Engineering, 5 (2017), pp. 3775-3785

I.M. Aroso, A.R. Araújo, R.A. Pires, R.L. Reis **Cork: Current technological developments and future perspectives for this natural, renewable, and sustainable material** ACS Sustainable Chemistry & Engineering, 5 (2017), pp. 11130-11146

E. Atanes, A. Nieto-Márquez, A. Cambra, M.C. Ruiz-Pérez, F. Fernández-Martínez **Adsorption of SO_2 onto waste cork powder-derived activated carbons** Chemical Engineering Journal, 211-212 (2012), pp. 60-67

K.K. Beltrame, A.L. Cazetta, P.S.C. de Souza, L. Spessato, T.L. Silva, V.C. Almeida, **Adsorption of caffeine on mesoporous activated carbon fibers prepared from pineapple plant leaves** Ecotoxicology and Environmental Safety, 147 (2018), pp. 64-71

B. Bestani, N. Benderdouche, B. Benstaali, M. Belhakem, A. Addou **Methylene blue and iodine adsorption onto an activated desert plant** Bioresource Technology, 99 (2008), pp. 8441–8444

I. Cabrita, B. Ruiz, A.S. Mestre, I.M. Fonseca, A.P. Carvalho, C.O. Ania **Removal of an analgesic using activated carbons prepared from urban and industrial residues** Chemical Engineering Journal, 163 (2010), pp. 249-255

B. Cardoso, A.S. Mestre, A.P. Carvalho, J. Pires **Activated carbon derived from cork powder waste by KOH activation: preparation, characterization, and VOCs adsorption** Industrial & Engineering Chemistry Research, 47 (2008), pp. 5841-5846

A.P. Carvalho, B. Cardoso, J. Pires, M.B. de Carvalho **Preparation of activated carbons from cork waste by chemical activation with KOH** Carbon, 41 (2003), pp. 2873-2884

A.P. Carvalho, M. Gomes, A.S. Mestre, J. Pires, M.B. de Carvalho **Activated carbons from cork waste by chemical activation with K_2CO_3. Application to adsorption of natural gas components** Carbon, 42 (2004), pp. 667-691

A.L. Cazetta, A.M.M. Vargas, E.M. Nogami, M.H. Kunita, M.R. Guilherme, A.C. Martins, T.L. Silva, J.C.G. Moraes, V.C. Almeida **NaOH-activated carbon of high surface area produced from coconut shell: kinetics and equilibrium studies from the methylene blue adsorption** Chemical Engineering Journal, 174 (2011), pp. 117-125

S. Cheng, L. Zhang, H. Xia, J. Peng, J. Shu, C. Li, X. Jiang, Q. Zhang **Adsorption behaviour of methylene blue onto waste-derived adsorbent and exhaust gases recycling** RSC Advances, 7 (2017), pp. 27331-27341

M. Demertzi, J.A. Paulo, L. Arroja, A.C. Dias **A carbon footprint simulation model for the cork oak sector** Science of the Total Environment, 566-567 (2016), pp. 499-511

E.N. El Qada, S.J. Allen, G.M. Walker **Adsorption of methylene blue onto activated carbon produced from steam activated bituminous coal: a study of equilibrium adsorption isotherm** Chemical Engineering Journal, 124 (2006), pp. 103-110

J. Febrianto, A.N. Kosasih, J. Sunarso, Y.-H Ju, N. Indraswati, S. Ismadji **Equilibrium and kinetic studies in adsorption of heavy metals using biosorbent: a summary of recent studies** Journal of Hazardous Materials, 162 (2009), pp. 616-645

K.Y. Foo, B.H. Hameed **Preparation, characterization and evaluation of adsorptive properties of orange peel based activated carbon via microwave induced K_2CO_3 activation** Bioresource Technology, 104 (2012), pp. 679-686

A. Galarneau, F. Villemot, J. Rodriguez, F. Fajula, B. Coasne **Validity of the t-plot method to assess microporosity in hierarchical micro/mesoporous materials** Langmuir, 30 (2014), pp. 13266-13274

P. Gao, Z.-H. Liu, G. Xue, B. Han, M.-H. Zhou **Preparation and characterization of activated carbon produced from rice straw by $(NH_4)_2HPO_4$ activation** Bioresource Technology, 102 (2011), pp. 3645-3648

L. Gil **Cork: a strategic material. Frontiers in Chemistry 2**, article 16 (2014), pp. 1-2

M. Goswami, P. Phukan **Enhanced adsorption of cationic dyes using sulfonic acid modified activated carbon** Journal of Environmental Chemical Engineering, 5 (2017), pp. 3508-3517

X. Han, H. Wang, L. Zhang **Efficient removal of methylene blue using nanoporous carbon from the waste biomass** Water, Air, & Soil Pollution, 229 (2018), pp. 26

Md. A. Islam, M.J. Ahmed, W.A. Khanday, M. Asif, B.H. Hameed **Mesoporous activated carbon prepared from NaOH activation of rattan (Lacosperma secundiflorum) hydrochar for methylene blue removal** Ecotoxicology and Environmental Safety, 138 (2017), pp. 279-285

M.I. Khan, T.K. Min, K. Azizli, S. Sufian, Z. Man, H. Ullah **Effective removal of methylene blue from water using phosphoric acid based geopolymers** RSC Advances, 5 (2015), pp. 61410-61420

S.-K. Kim **Springer handbook of marine biotechnology**. Springer-Verlag Berlin Heidelberg, (2015), ISBN: 978-3-642-53971-8.

Z. Li, G. Wang, K. Zhai, C. He, Q. Li, P. Guo **Methylene blue adsorption from aqueous solution by loofah sponge-based porous carbons** Colloids and Surfaces A: Physicochemical and Engineering Aspects, 538 (2018), pp. 28-35

X. Ma, F. Ouyang **Adsorption properties of biomass-based activated carbons prepared with spent coffee grounds and pomelo skin by phosphoric acid activation** Applied Surface Science, 268 (2013), pp. 566-570

A.S. Mestre, J. Pires, J.M.F. Nogueira, A.P. Carvalho **Activated carbons for the adsorption of ibuprofen** Carbon, 45 (2007), pp. 1979-1988

A.S. Mestre, R.A. Pires, I. Aroso, E.M. Fernandes, M.L. Pinto, R.L. Reis, M.A. Andrade, J. Pires, S.P. Silva, A.P. Carvalho **Activated carbons prepared from industrial pre-treated cork: sustainable adsorbents for pharmaceutical compounds removal** Chemical Engineering Journal, 253 (2014), pp. 408-417

S. Naeem, V. Baheti, J. Wiener, J. Marek **Removal of methylene blue from aqueous media using activated carbon web** The Journal of the Textile Institute, 108 (2017), pp. 803-811

A. Nasrullah, A.H. Bhat, A. Naeem, M.H. Isa, M. Danish **High surface area mesoporous activated carbon-alginate beds for efficient removal of methylene blue** International Journal of Biological Macromolecules, 107 (2018), pp. 1792-1799

R.M. Novais, G. Ascensão, D.M. Tobaldi, M.P. Seabra, J.A. Labrincha **Biomass fly ash geopolymer monoliths for effective methylene blue removal from wastewaters** Journal of Cleaner Production, 171 (2018), pp. 783-794

D. Pathania, S. Sharma, P. Singh **Removal of methylene blue by adsorption onto activated carbon developed from Ficus carica bast** Arabian Journal of Chemistry, 10 (2017), pp. S1445-S1451

Z. Peng, Z. Guo, W. Chu, M. Wei **Facile synthesis of high-surface area activated carbon from coal for supercapacitor and high CO_2 sorption** RSC Advances, 6 (2016), pp. 42019-42028

H. Pereira, 2007. **Cork: Biology, Production and Uses**. first ed. Elsevier B.V, Amsterdam. ISBN: 9780080476865.

A.M.A Pintor, C.I.A. Ferreira, J.C. Pereira, P. Correia, S.P. Silva, V.J.P. Vilar, C.M.S. Botelho, R.A.R. Boaventura **Use of cork powder and granules for the adsorption of pollutants: a review** Water Research, 46 (2012), pp. 3152-3166

A.M.A. Pintor, A.M. Silvestre-Albero, C.I.A. Ferreira, J.P.C. Pereira, V.J.P. Vilar, C.M.S. Botelho, F. Rodríguez-Reinoso, R.A.R. Boaventura **Textural and surface**

characterization of cork-based sorbents for the removal of oil from water Industrial & Engineering Chemistry Research, 52 (2013), pp. 16427-16435

R.C. Pullar, P. Marques, J. Amaral, J.A. Labrincha **Magnetic wood-based biomorphic $Sr_3Co_2Fe_{24}O_{41}$ Z-type hexaferrite ecoceramics made from cork templates** Materials and Design, 82 (2015), pp. 297-303

R.C. Pullar, R.M. Novais **Ecoceramics: cork-based biomimetric ceramic 3-DOM foams** Materials Today, 20 (2017), pp. 45-46

M. Rafatullah, O. Sulaiman, R. Hashim, A. Ahmad **Adsorption of methylene blue on low-cost adsorbents: a review** Journal of Hazardous Materials, 177 (2010), pp. 70-80

F. Raposo, M.A. Rubia, R. De La Borja **Methylene blue as useful indicator to evaluate the adsorptive capacity of granular activated carbon in batch mode: influence of adsorbate/adsorbent mass ratio and particle size** Journal of Hazardous Materials, 165 (2009), pp. 291-299

S. Sangon, A.J. Hunt, T.M. Attard, P. Mengchang, Y. Ngernyen, N. Supanchaiyamat **Valorisation of waste rice straw for the production of highly effective carbon based adsorbents for dyes removal** Journal of Cleaner Production, 172 (2018), pp. 1128-1139

K.S.W. Sing, D.H. Everett, R.A.W. Haul, L. Moscou, R.A. Pierotti, J. Rouquérol, T. Siemieniewska **Reporting physisorption data for gas/solid systems with special reference to the determination of surface area and porosity** Pure & Applied Chemistry, 57 (1985), pp. 603–619

G.G. Stavropoulos, A.A. Zabaniotou **Production and characterization of activated carbons from olive-seed waste residue** Microporous and Mesoporous Materials, 82 (2005), pp. 79–85

H.N. Tran, S.-J. You, H.-P. Chao **Fast and efficient adsorption of methylene green 5 on activated carbon prepared from new chemical activation method** Journal of Environmental Management, 188 (2017), pp. 322-336

A.M.M. Vargas, A.L. Cazetta, M.H. Kunita, T.L. Silva, V.C. Almeida **Adsorption of methylene blue on activated carbon produced from flamboyant pods (Delonix regia): study of adsorption isotherms and kinetic models** Chemical Engineering Journal, 168 (2011), pp. 722-730

M.T. Vu, H.-P. Chao, T.V. Trinh, T.T. Le, C.-C. Lin, H.N. Tran **Removal of ammonium from groundwater using NaOH-treated activated carbon derived from corncob wastes: batch and column experiments** Journal of Cleaner Production, 180 (2018) pp. 560-570

K.T. Wong, N.C. Eu, S. Ibrahim, H. Kim, Y. Yoon, M. Jang **Recyclable magnetite-loaded palm shell-waste based activated carbon for the effective removal of methylene blue from aqueous solution** Journal of Cleaner Production, 115 (2016), pp. 337-342

World Economic Forum. The global risks report 2016. 11 Edition. Geneva, Switzerland: World Economic Forum, 2016. Available from: www3.weforum.org/docs/GRR/WEF_GRR16.pdf (accessed on 01.06.18).

K. Yang, J. Peng, C. Srinivasakannan, L. Zhang, H. Xia, X. Duan **Preparation of high surface area activated carbon from coconut shells using microwave heating** Bioresource Technology, 101 (2010), pp. 6163-6169

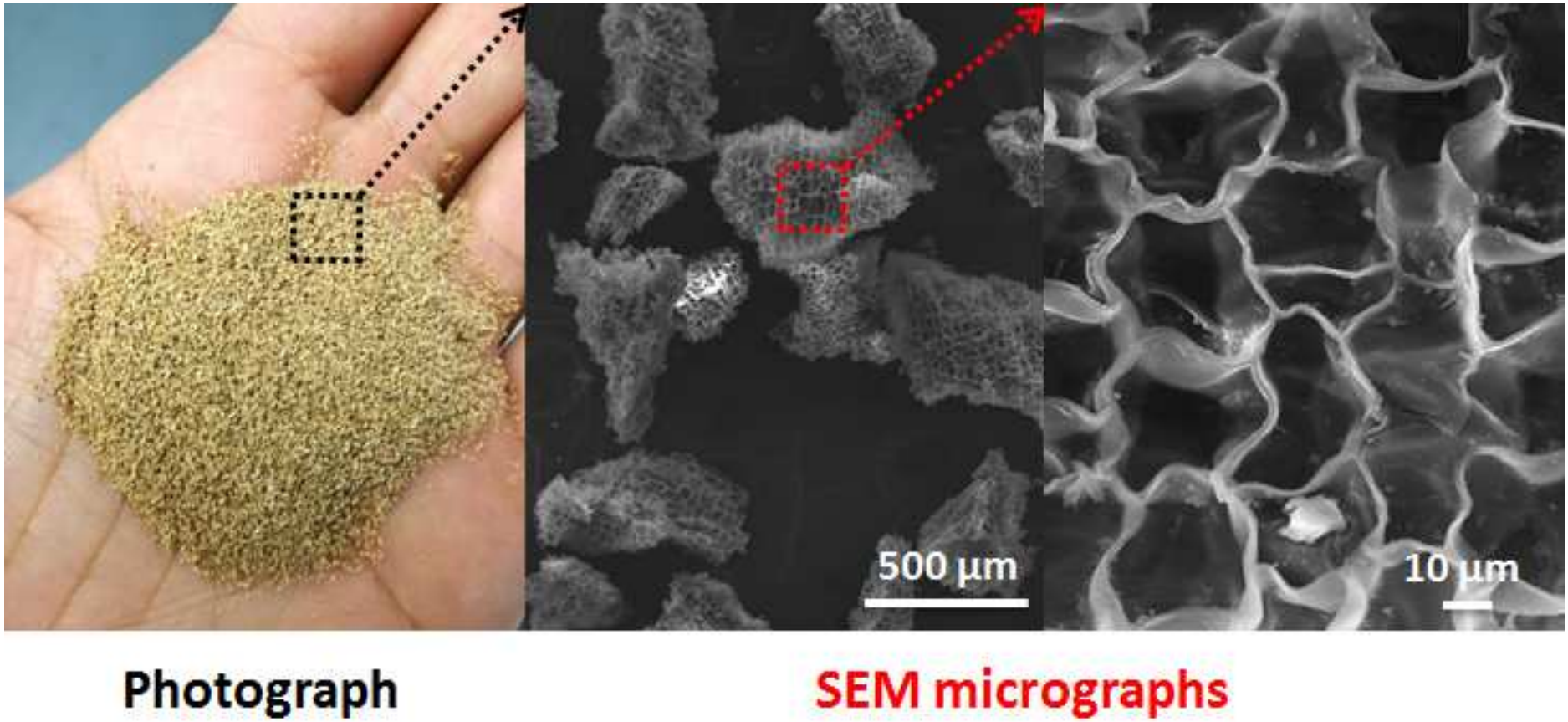

Fig. 1 Photograph of the cork powder waste produced during the corks granulation process, and SEM micrographs of the cork powder.

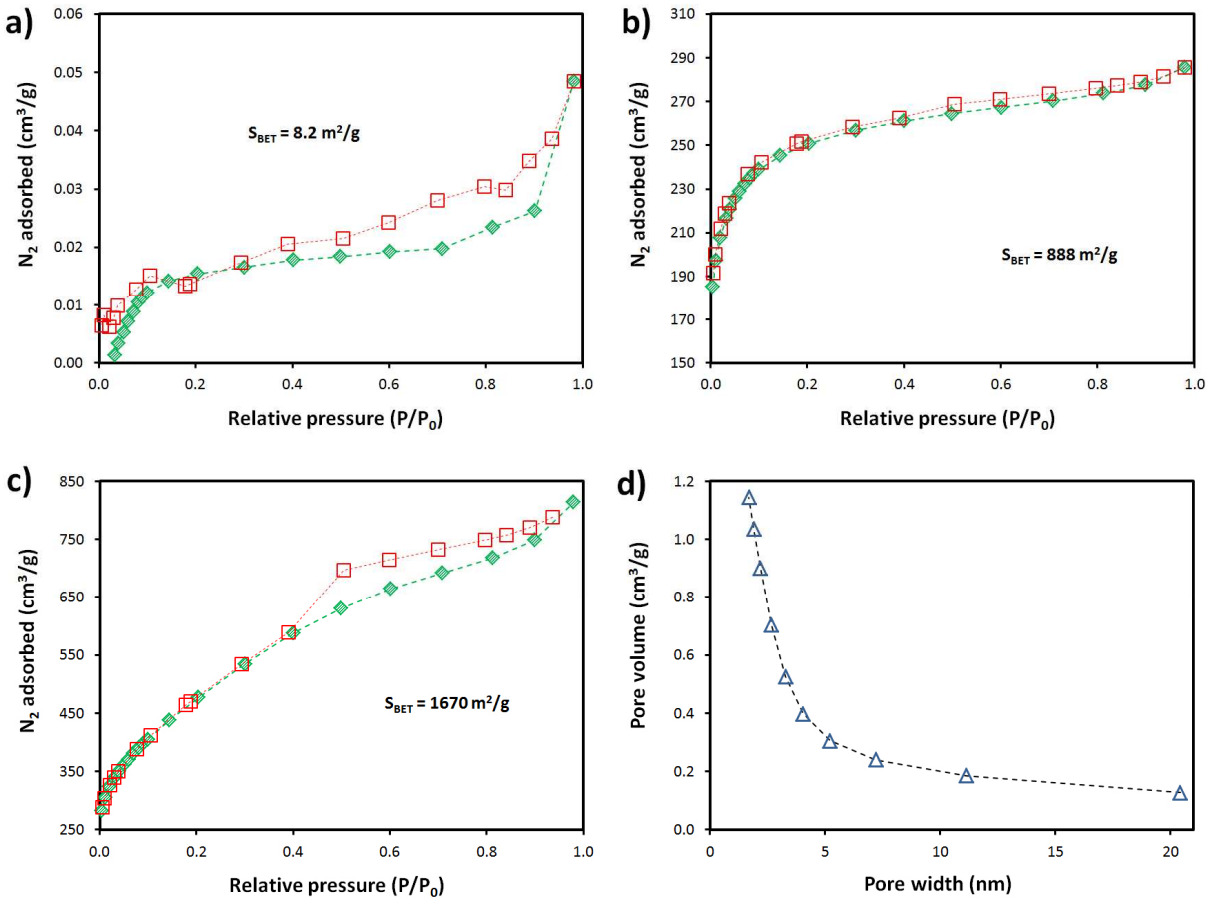

Fig. 2 N_2 adsorption (green diamonds) and desorption (red squares) isotherms (a-c) of the a) *as-received* cork powder and the activated carbon synthesised using an wastewater:NaOH ratio of b) 75: 25 vol.% and c) 50: 50 vol.%. Fig. 2d presents the cumulative pore volume of the AC adsorbent corresponding to the ratio of 50: 50 vol.%. The BET surface area calculated from the N_2 adsorption isotherm is included in Fig. 2a-c.

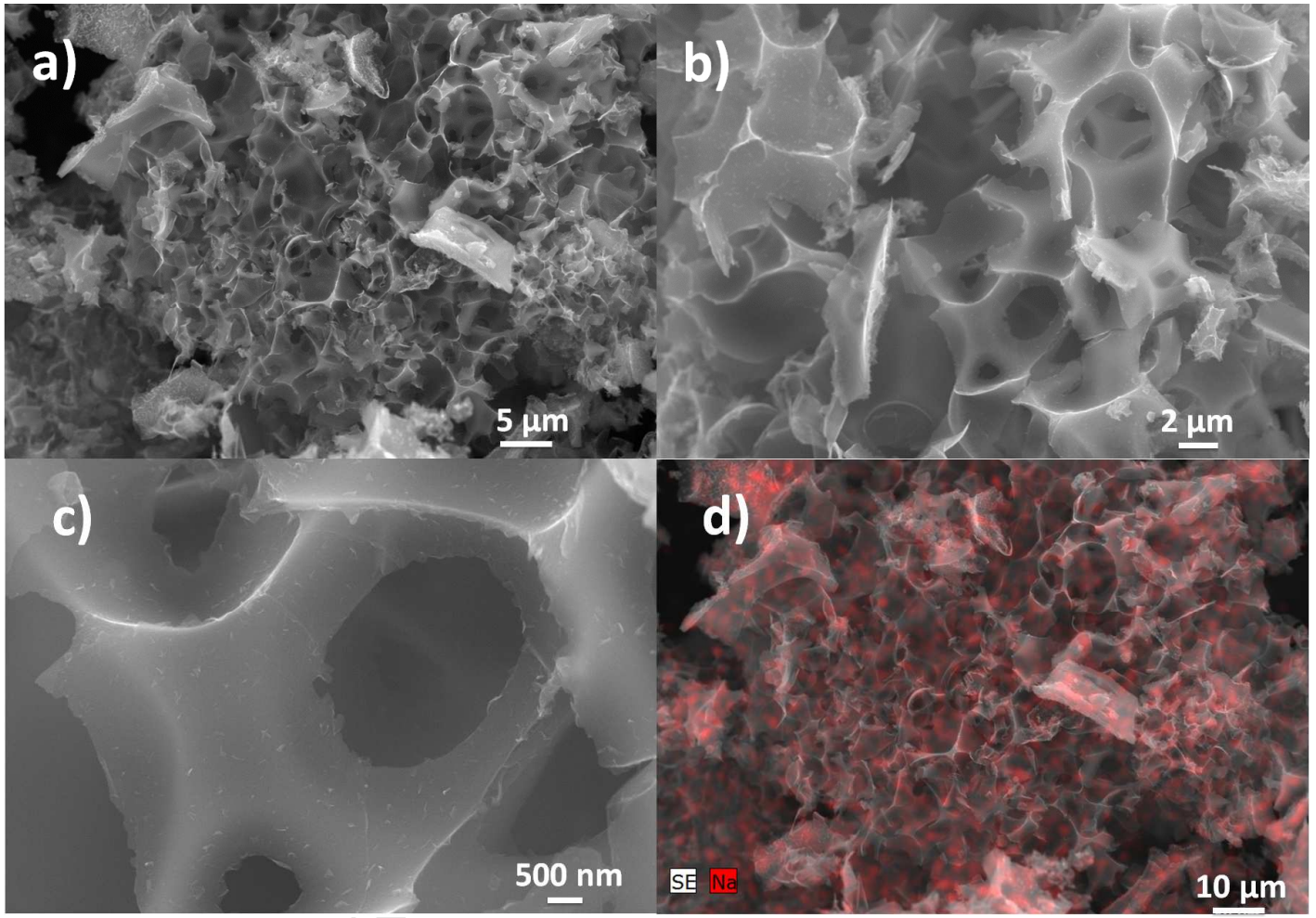

Fig. 3 SEM micrographs at various magnifications (a-c) and EDS elemental mapping (d) of the activated carbon prepared using a mixture of 50 vol.% each of wastewater and NaOH as activators.

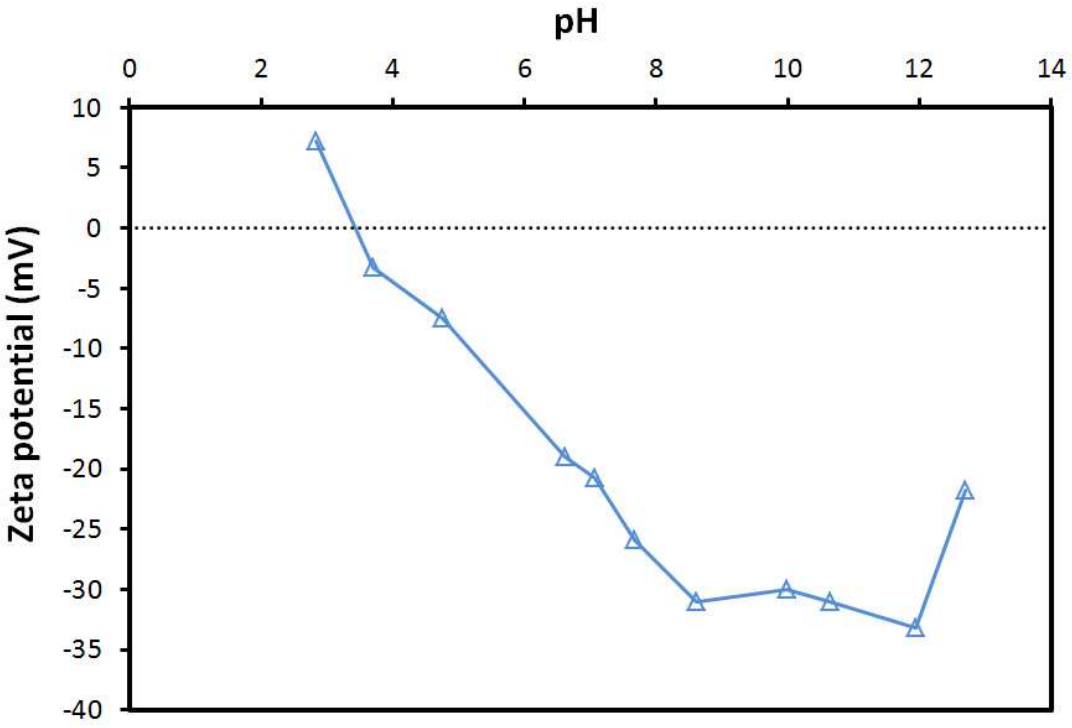

Fig. 4 Activated carbon zeta potential evolution with pH (measured at room temperature).

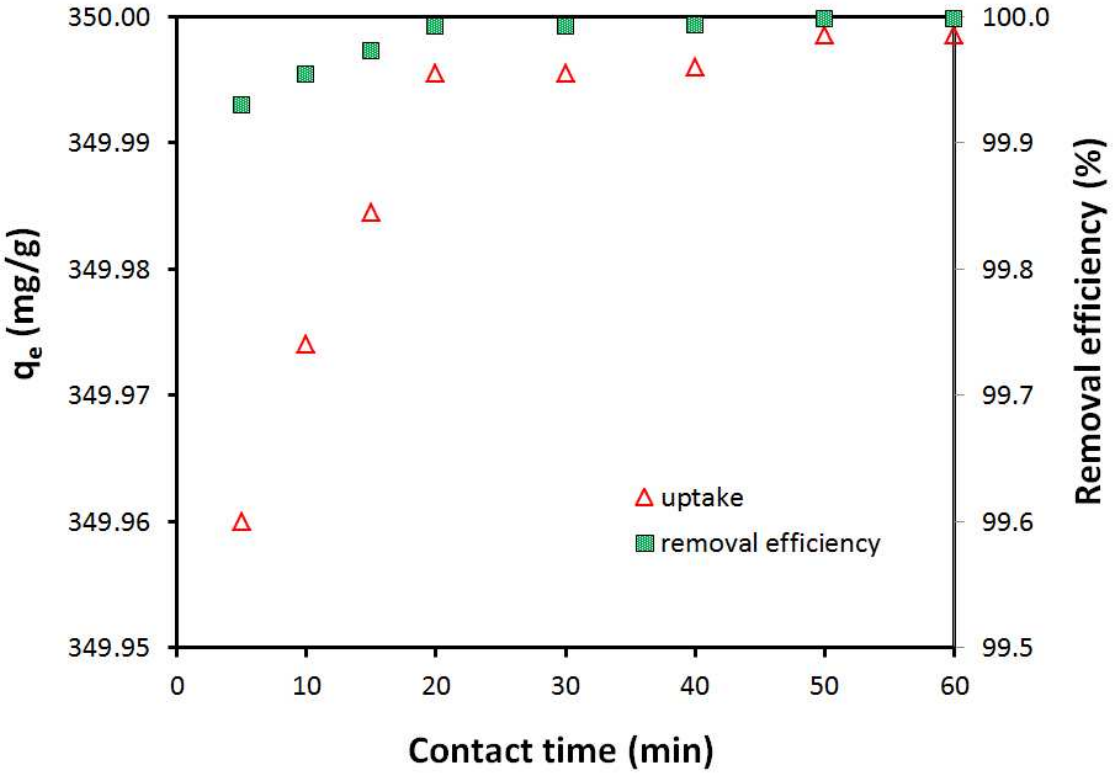

Fig. 5 Influence of contact time on the uptake and removal efficiency of methylene blue by the activated carbon (adsorbent dose: 2 g/L; C_0 = 700 ppm; T = 20 ºC).

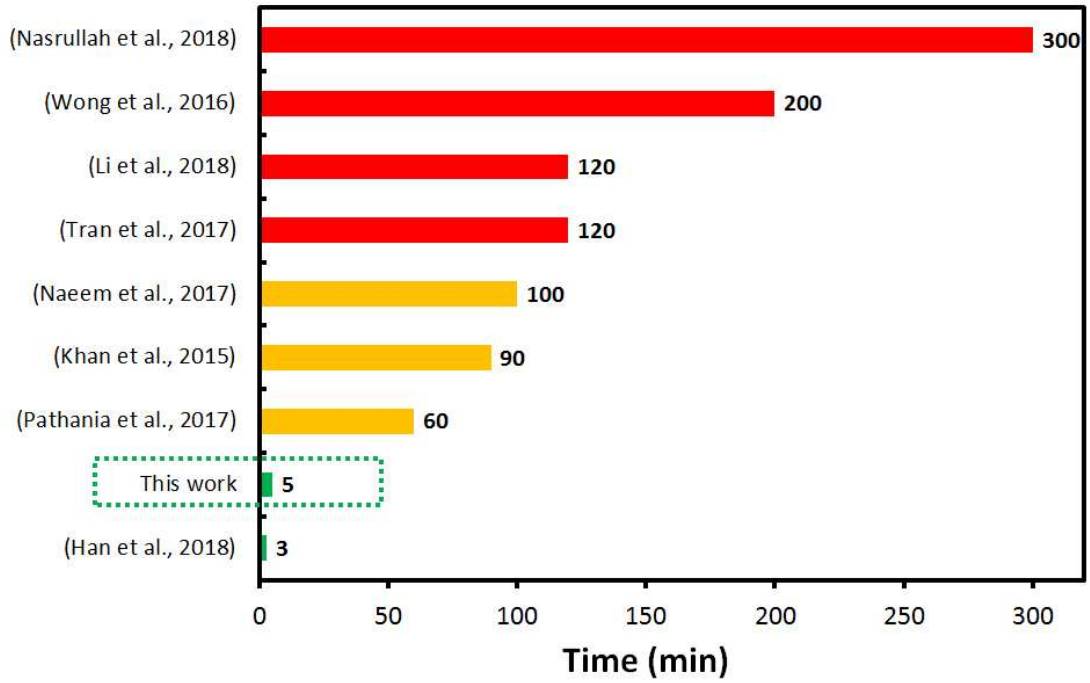

Fig. 6 Equilibrium time of various MB adsorbents reported in the literature. Red bars correspond to equilibrium times above 100 min, orange bars between 60 and 100 min, and green bars below 10 min.

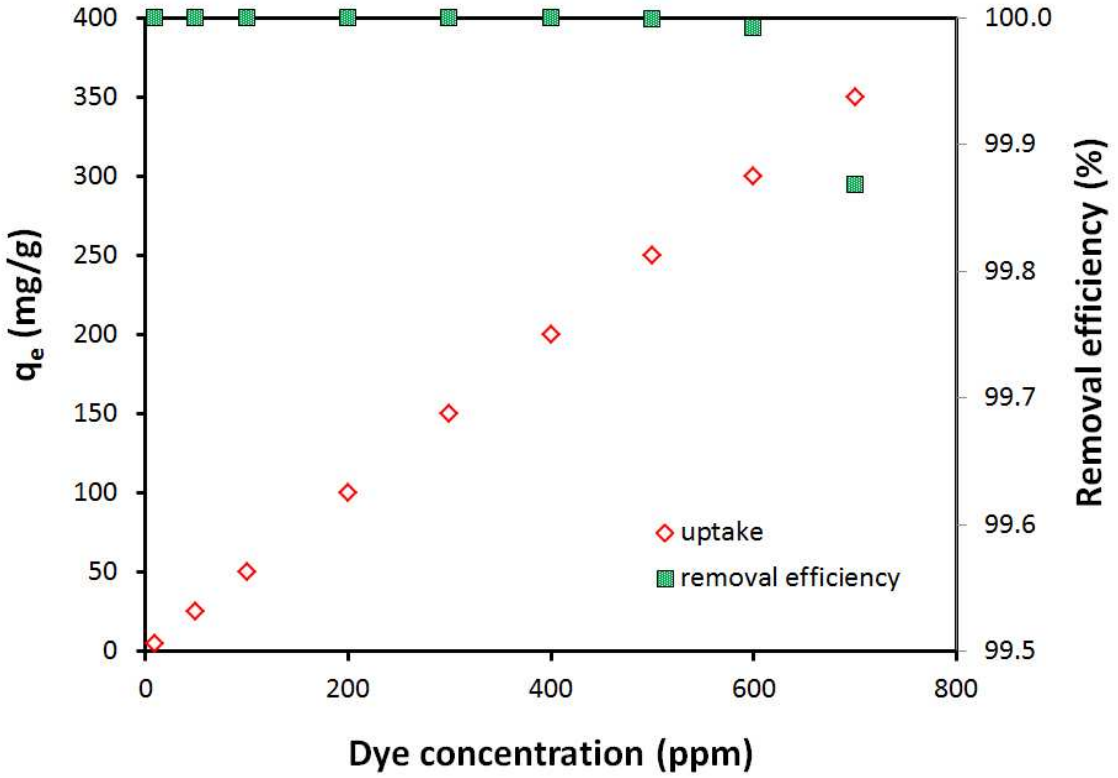

Fig. 7 Influence of methylene blue initial concentration on the uptake and removal efficiency of this pollutant by the activated carbon (adsorbent dose: 2 g/L; contact time: 10 min; T = 20 ºC).

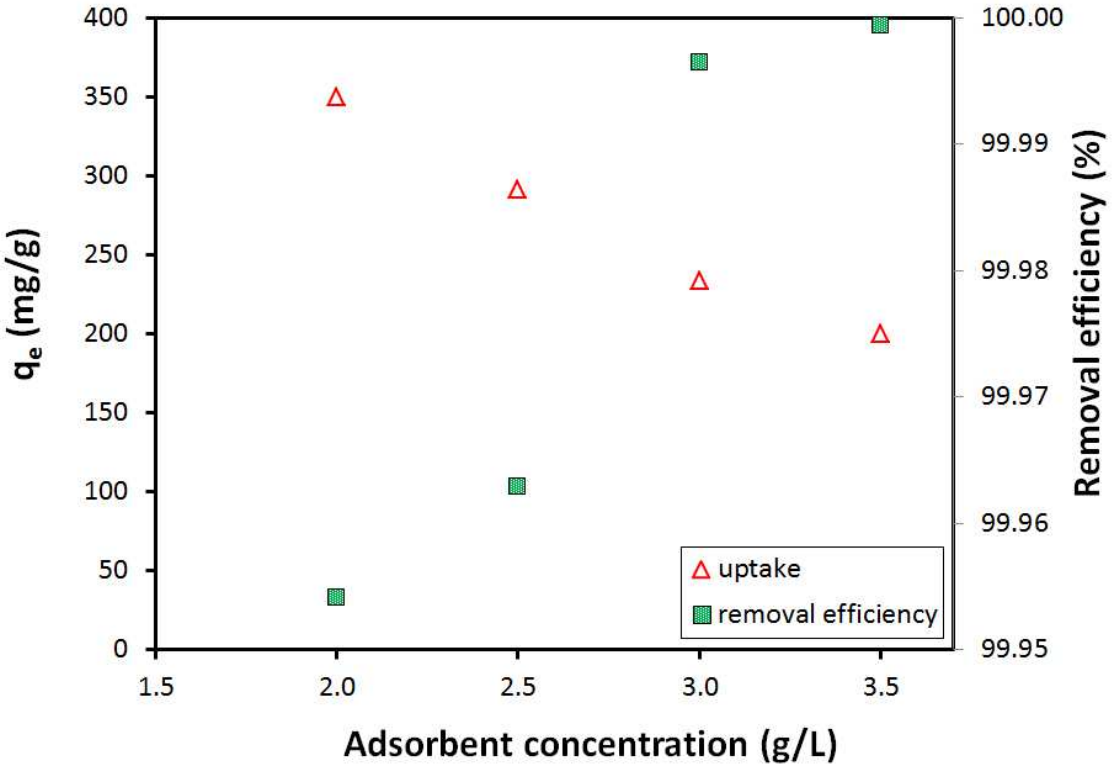

Fig. 8 Influence of the AC concentration on the uptake and removal efficiency of methylene blue (contact time: 10 min; C_0 = 700 ppm; T = 20 ºC).

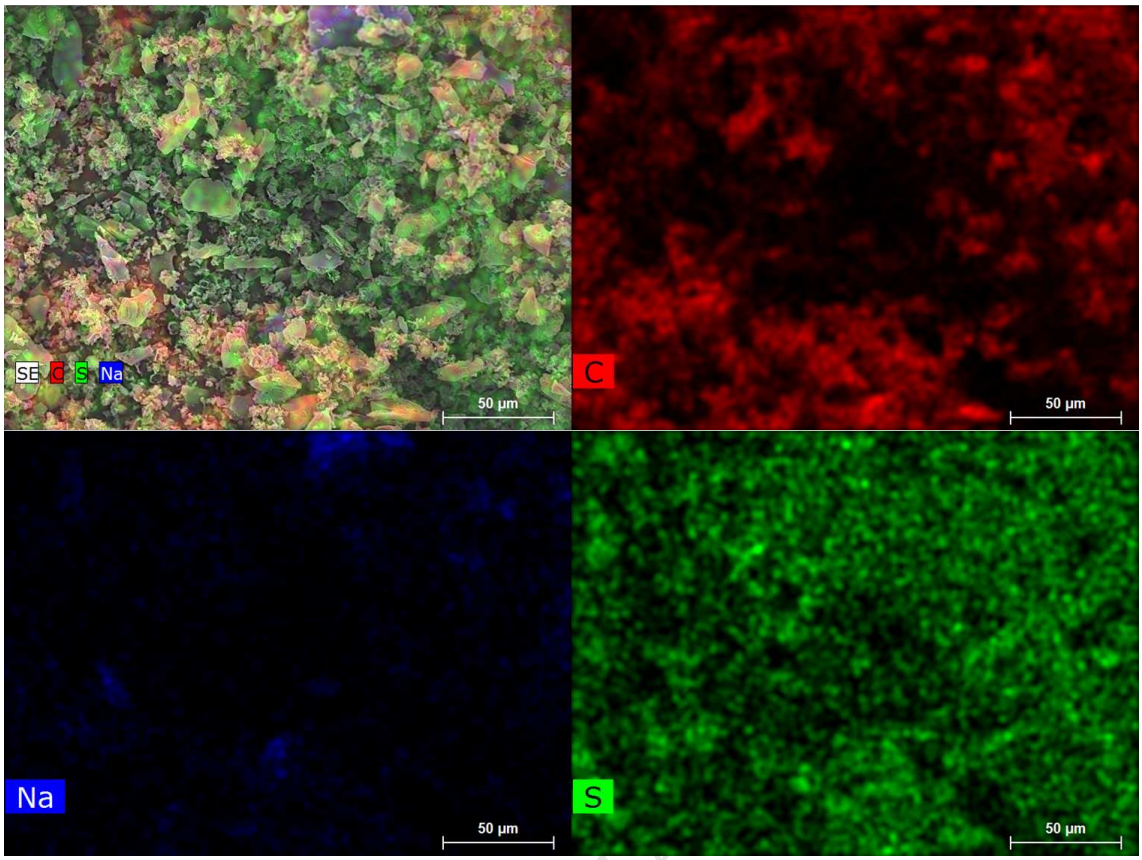

Fig. 9 EDS elemental mapping of the activated carbon after MB adsorption tests (contact time: 10 min; C_0 = 700 ppm; T = 20 ºC).

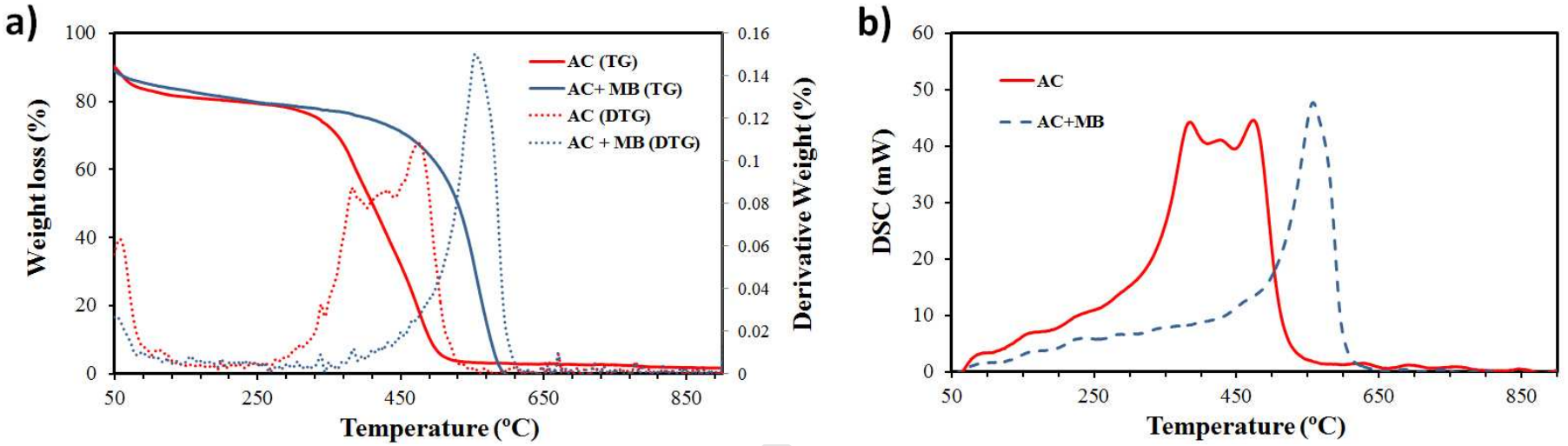

Fig. 10 a) TG and b) DSC curves of activated carbon (AC) before and after MB adsorption tests.

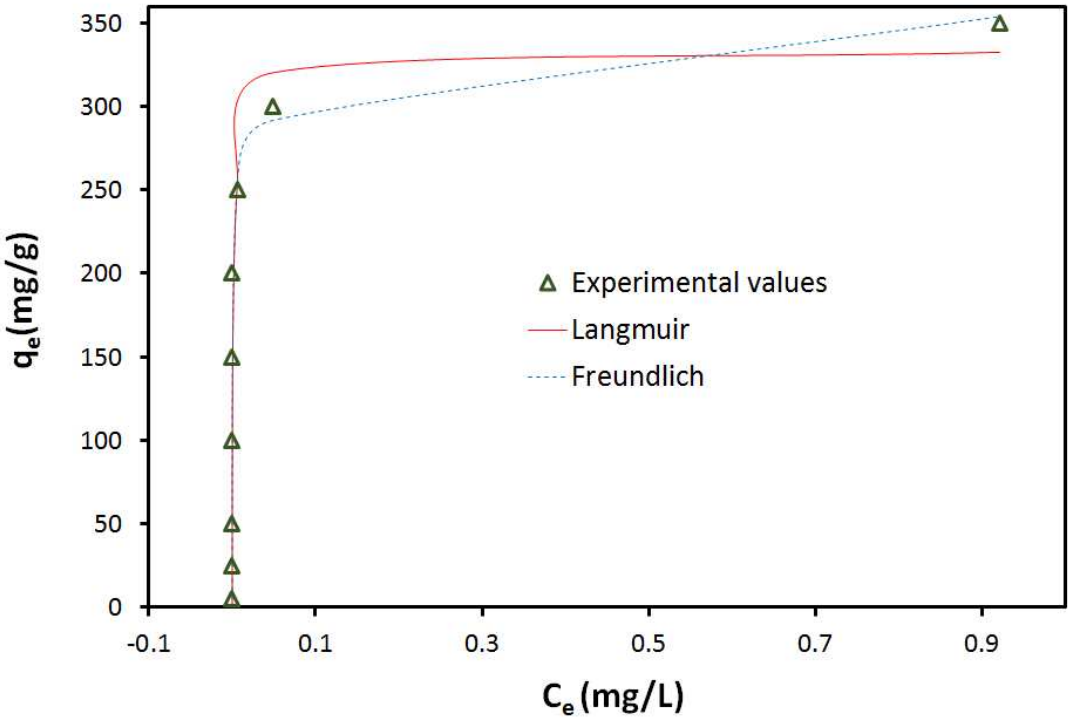

Fig. 11 Fits of the Langmuir and the Freundlich isotherms.

Table 1 Physical properties of the activated carbon used in this study (synthesised using a wastewater:NaOH ratio of 50:50 vol.%).

	Activated carbon
Total surface area (BET) (m^2/g)	1670
Micro surface area (m^2/g)	117.3
Total pore volume (cm^3/g)	1.14
Micropore volume (cm^3/g)	0.06
Mean particle size (µm)	29.8
pH_{PZC}	3.6
Contact angle (º)	34.9

Table 2 Specific surface area (BET) and activation method of various adsorbents (green highlighted: Cork-based activated carbons).

Material	Activation method	Total surface area (BET) (m^2/g)	Reference
Acrylic fibrous waste	Physical activation (air)	280	(Naeem *et al.*, 2017)
Waste cork powder	KOH	584	(Atanes *et al.*, 2012)
Bituminous coal	Steam activation	857	(Qada *et al.*, 2006)
Waste cork powder	K_2CO_3	891	(Cabrita *et al.*, 2010)
Granules of expanded corkboard	KOH	948	(Mestre *et al.*, 2014)
Pineapple leaf fibres	H_3PO_4	1031	(Beltrame *et al.*, 2018)
Waste cork powder	K_2CO_3	1060	(Mestre *et al.*, 2007)
Corncob wastes	H_3PO_4 + NaOH (treatment after pyrolysis)	1097	(Vu *et al.*, 2018)
Orange peel	K_2CO_3	1104	(Foo and Hameed, 2012)
Rattan	NaOH	1165	(Islam *et al.*, 2017)
Tea leaf	H_3PO_4	1169	(Goswami and Phukan, 2017)
Waste cork	K_2CO_3	1279	(Carvalho *et al.*, 2004)
Waste carbon	Ultrasonic spray	1312	(Cheng *et al.*, 2017)
Waste cork powder	KOH	1336	(Cardoso *et al.*, 2008)
Waste cork	H_2SO_4 (pre-treatment) + KOH	1415	(Carvalho *et al.*, 2003)
Mangosteen peels	$ZnCl_2$	1622	(Nasrullah *et al.*, 2018)
Waste cork powder [a]	**Alkaline wastewater and NaOH (50 vol.%)**	**1670**	**-**
Waste rice straw	KOH	1973	(Sangon *et al.*, 2018)
Coconut shells	Microwave heating and CO_2 activation	2288	(Yang *et al.*, 2010)
Coal	KOH	2457	(Peng *et al.*, 2016)
Coconut shell	NaOH	2825	(Cazetta *et al.*, 2011)

[a] The font in bold identifies the results obtained in this work.

Table 3 Maximum MB adsorption capacity (mg/g) of various adsorbents (grey highlighted: uptakes below 100 mg/g; orange highlighted: uptakes between 100 and 300 mg/g; green highlighted: adsorptions greater than 300 mg/g). For comparison purposes the temperature of the adsorption test was also included in the table.

Material	Temperature (ºC)	Maximum MB adsorption capacity (mg/g)	Reference
Bituminous coal	Not given	580	(Qada *et al.*, 2006)
Wheat straw	20	556	(Han et al., 2018)
Waste rice straw	Room temperature	528	(Sangon *et al.*, 2018)
Waste cork powder [a]	20	350	-
Waste carbon	50	290	(Cheng et al., 2017)
Filtrasorb 300 (commercial)	Not given	240	(Stavropoulos and Zabaniotou, 2005)
Mangosteen peels	Room temperature	230	(Nasrullah *et al.*, 2018)
Loofah sponge	30	211	(Li et al., 2018)
Merck activated carbon (commercial)	Room temperature	200	(Bestani et al., 2008)
Palm shell	Not given	163	(Wong et al., 2016)
Rice straw	Not given	130	(Gao et al., 2011)
Ficus carica bast	30	48	(Pathania et al., 2017)
Biomass fly ash geopolymer	20	15	(Novais et al., 2018)
Acrylic fibrous waste	25	9	(Naeem *et al.*, 2017)

[a] The font in bold identifies the results obtained in this work.

Table 4 Langmuir and Freundlich parameters for MB adsorption by the cork-based activated carbon.

Sample	Langmuir			Freundlich		
	q_m (mg/g)	K_L (L/mg)	R^2	K_F (L/g)	*1/n*	R^2
AC	333.33	500.00	0.902	355.96	0.066	0.979

Highlights

- Eco-friendly cork waste-based activated carbons were successfully synthesised.
- Cork chemically activated for the first time using alkaline industrial wastewater.
- Highest ever reported specific surface area for activated cork carbons, 1670 m^2/g.
- For the first time cork-based activated carbons were evaluated as MB adsorbents.
- Fast (>99.9% removal in 5 min) and efficient (350 mg/g) MB extraction was achieved.